Numerical Simulation of Impact and Penetration of Ogvial Shaped Projectiles through Steel Plate Structures

Damith Mohotti
(p.jayasekaramohotti@student.unimelb.edu.au)
Tuan Ngo
(dtngo@unimelb.edu.au)
Priyan Mendis
((pamendis@unimelb.edu.au)
Department of Infrastructure Engineering, The University of Melbourne

Abstract

There is an urgent need to develop light-weight protective structures with a sufficient protection to prevent the damage occurring during extreme loading events such as blast and ballistic impacts. This study is a part of ongoing research to develop light weight amour materials which can sustain under those severe conditions. Numerical modelling with explicit finite element code LS-DYNA has performed with realistic geometries. Ballistic protection class BR7 in European norm EN 1063 considered, thus penetration of different shaped projectiles through thick steel plates was examined. Since the geometries and materials of the projectiles have a very significant influence on the outcome of this research detail modelling of the projectiles was performed. For the purpose of this paper, perforation mechanism of 7.62mm APM2 bullet through 6mm thick Weldox 460E high strength structural steel plate was examined. Largrangian methods combined with Johnson-Cook material model available in the LS-DYNA were used for the numerical simulations. Finally the ballistic limit curve for the 6mm thick Weldox 460E plate perforated by APM2 bullet was obtained. Results were compared with the analytical models.

Keywords: high-strength steel, ballistic impact, modified Johnson-Cook model

1 Introduction

Numerical simulations play a vital role in modern protective amour design industry as it save time as well as cost by reducing the number repetitive field tests. With the advancement of the finite element design codes such as LS-DYNA it is reliable to calibrate a model with actual test data and use those validated parameters for the similar future works.

Different researches have being conducted to obtain the ballistic limit curves for various materials over the years. With the advancement of the computer capabilities, it is now possible to perform a numerical simulation within reasonable time frame to satisfactorily obtain the reliable results.

Though there are large number of innovative materials develops over the years, steel is the foremost material in the context of protective amours (Børvik et al., 2009). Penetration and failure mechanisms of thick steel plates by different shaped projectiles are considered here. Backman and Goldsmith have highlighted eight modes of perforation mechanisms related to ductile and brittle targets. Perforation mechanism depends on projectile nose shape, impact velocity, target property, target thickness and size. For an example this can be a ductile hole enlargement for a conical shaped projectile and plugging for a blunt shaped projectile etc. (Chen et al., 2003).

Most commonly used parameter to identify the targets capability to withstand the projectile impact is the ballistic limit velocity. Ballistic limit velocity is the maximum velocity that a projectile can travel without fully penetrating a particular structure. This is a unique parameter for a structure as well as for a projectile. Analytical, numerical and experimental models have been developed to obtain the ballistic limit over the years.

One of the limitations of the most of previous researches is the lack of detailing in the modelling of projectile. Since shape of the projectile plays a vital role on the failure mechanism it is important to develop the numerical models with realistic geometries and materials. Thus make it possible to validate with experimental or analytical results with greater accuracy. Material behaviour of the projectile also has influence on the failure mechanism hence the usage of authentic material parameters for the analysis is a prime importance. Horsfall et al. (2000) has compared four variations of APM2 bullet penetration through a similar target and has come to a conclusion that the design of the projectile has a very high influence to its performance.

The main focus of the paper is to present a comprehensive work on the numerical modeling of 7.62x63mm APM2 bullet penetration through a 6mm thick Weldox 460E steel plate and development of ballistic limit curve for the plate and the projectile. Chen and Li analytical models are briefly discussed in order to validate the numerical model results.

2 Analytical Method

The analytical models that develop over the years could be classified in to three main categories such as models that predict local deformation and failure, global deformation and failure or both (Corbett et

al., 1996). It has understood that fairly simple analytical model can predict the target response to certain accuracy but to obtain an accurate result more complex models are a requirement. Focus of this paper has given to the model proposed by Chen and Li.

Chen and Li (2003) has developed an analytical model based on dynamic cavity expansion theory which considers hole enlargement for sharp projectile nose and the plugging formation for a blunt projectile nose. The models have developed for non deformable projectile with thick plates. It has assumed materials behave as elastic-perfectly plastic material or incompressible elastic, strain-hardening plastic material. Local effect becomes an important parameter when the thickness of the plate gets increased.

For the projectile with sharp nose as given in Figure 1(a) the ballistic velocity V_{bl} can be expressed as,

$$V_{bl} = \left[\frac{AN_1\sigma_y}{BN_2\rho}\left\{exp\left(\frac{\pi\chi}{2N^*}\right) - 1\right\}\right]^{1/2} \quad (1)$$

for h/d ,

$$\frac{h}{d} \geq \frac{\sqrt{3}AN_1(1 + l/N)}{4\, exp\left[\frac{\pi\chi}{2N^*}\right]} \quad (2)$$

Where h and d are the nose height and diameter of the projectile. σ_y is yield stress and N_1 and N_2 are dimensionless parameters. If the friction is ignored from the calculations $N_1=1$ and $N^*=N_2$ (Chen et al., 2002).

Nose shape parameter for ogive nose N^* is given by,

$$N^* = \frac{1}{3\psi} - \frac{1}{21\psi^2} \quad (3)$$

$$\psi = x/d \quad (4)$$

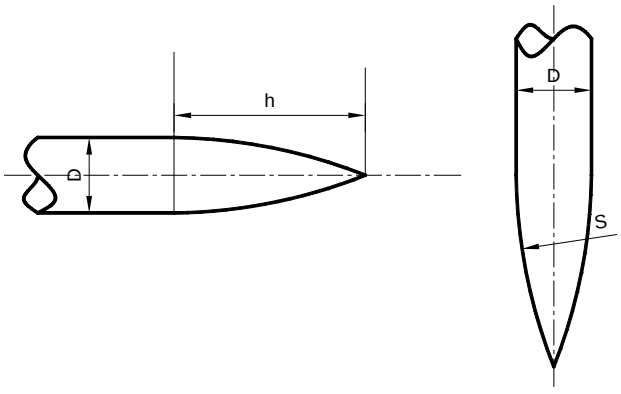

(a) (b)

Figure 1: (a) (b) Ogive nose projectile

The dimensionless thickness of the plate is the ratio between plate thickness, h and the nose diameter, d and given by,

$$\chi = \frac{h}{d} \quad (5)$$

Assuming target material as a perfect elastic-plastic material for the simplicity dimensionless parameter A can be given by,

$$A = \frac{2}{3}\left\{1 + \ln\left[\frac{E}{3(1-\gamma)\sigma_y}\right]\right\} \quad (6)$$

Where E is young's modulus, and γ is the Poisson's ratio.

3 Development of the Numerical Models

The impact of the projectiles with the 6mm armour steel was simulated using the advanced FE code LS-DYNA (Ls Dyna Keyword User's Manual, in Version 971. 2007). Geometry and the mesh for the projectiles were modelled in ANSYS work bench and ANSYS CFD 12.1 and exported to LS-PREPOST for further developments. The numerical model development process is discussed in the following sections in detail.

The geometries of the bullets are given in Figure 2. The dimension of the 7.62mmx63mm APM2 bullet extracted from the published literatures. AMP2 bullet consists of four distinguished parts with a brass outer cover, brass cap, hardened steel inner core and a lead fill.

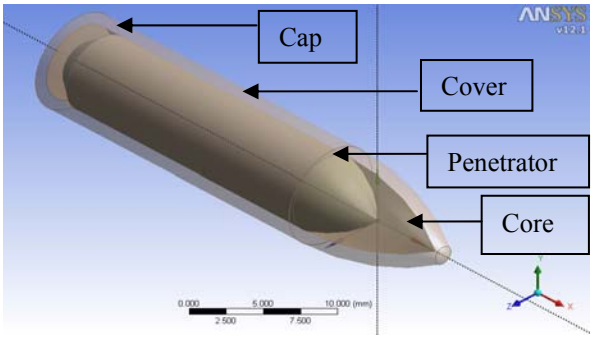

Figure 2: Geometry 7.62x51mm AMP2 bullet

APM2 bullets modelled with tetrahedral elements. A quarter models were used for the analysis to save the computation time for the tetrahedral model. The APM2 geometry was meshed with 42,351 number of tetrahedron elements in ANSYS Mechanical platform with 0.2mm maximum edge length. The mesh quality was one of the key parameters considered here since it could have high influence on the analysis results. "Skewness" of the elements was in the range of 0-0.80 thus achieved a quality mesh. Plate with dimensions 120mm x 120mm x 12mm has been modelled with 270,000 solid elements by achieving the aspect ratios of 1 in the critical areas and the 2 in the remaining areas.

Constant stress solid elements were assigning to the plate while single point tetrahedron elements were assigned to the plate. Contact was defined using the key word *CONTACT_ERRODING SURFACE TO SURFACE.

4 Material models

4.1 Johnson-Cook Constitutive Model

Materials under goes high strain and large strain rate deformation due to an impact such as projectiles. The material deformation process under these dynamic loadings is far remote from the qausi-statistic and low-strain rate conditions (Odeshi et al., 2005). Due to this high strain rate deformation local rise in the temperature occurs and it is called adiabatic heating. Adiabatic heating cause softening in the material locally and the effect of it is higher than the strain-hardening effect. It is important to select a material model which can be used to trace these effects during the numerical analysis. Model developed by Johnson and Cook (Johnson et al.) takes the consideration of strain rate effect, strain hardening effect and the temperature effect of the materials behave under different strain rate loadings. LS-DYNA v971 uses three versions of Johnson-Cook material models which can be used with steel materials deforming under different strain rates. The Key word *MAT MODIFIED JOHNSON-COOK (MJC) (Ls Dyna Keyword User's Manual, in Version 971. 2007) has been used in the numerical simulations as it is the most comprehensive model of them all. The advantage of using this model is, it has several alternative paths that user can use when defining the constitutive relationship and fracture criteria of the materials, which can predict the physical behaviour of the projectile impact to a reasonable accuracy (Børvik et al., 2009; Adams, 2003).

MJC model defined the material strength σ_y by,

$$\sigma_y = [A + Br^n](1 + \dot{r}^*)(1 - T^m) \tag{7}$$

Where r is equivalent plastic strain rate, $\dot{r}^*$ is normalized damage-equivalent plastic strain rate. The normalized damage-equivalent plastic strain rate is the ratio between a particular strains rated to a user defined strain rate as given in Eq.(8).

$$\dot{r}^* = \frac{\dot{r}}{\dot{\varepsilon}_0} \tag{8}$$

A,B,n and m are material constants which can be obtain from different tests. The homologous temperature T^* is given by,

$$T^* = \frac{T - T_r}{T_m - T_r} \tag{9}$$

Subscripts m and r stands for melting temperature and the room temperature. The temperature rise, ΔT due to adiabatic heating can be calculated as,

$$\dot{\Delta T} = \chi \frac{\dot{\sigma}_{eq}{}^{\wedge}}{\rho C_p} \quad (10)$$

Where, χ is the Taylor-Quinney parameter, ρ is the density and C_p is the specific heat of the materials. The initial value of the temperature shall be defined by the user. The advantage of using the MCJ material model is user has choice to select the constitutive relationship from either Johnson-Cook or Zerilli-Armstrong relationship. In this study Johnson-Cook model was used as the constitutive relationship for all the materials except lead. The MCJ parameter used for the analysis is tabulated and present in Table **1**.

Table 1: MCJ model material parameters

Material	*A*	*B*	*n*	*C*	*m*	*Tr*	*Tm*	$\dot{\varepsilon}_0$
	(MPa)	*(MPa)*	-	-	-	*(K)*	*(K)*	*(S^{-1})*
Brass cover/cap	206	505	0.42	0.01	1.67	293	1189	5E-04
Hardened inner core (APM2)	1200	50000	1.0	0	1.0	293	1800	5E-04
Weldox 460E plate	499	382	0.458	0.0079	0.893	293	1800	5E-04

4.2 Steinburg-Guinan Model

Lead is a dense ductile, very soft and highly malleable metal which has a melting temperature around 600(K). During the projectile impact the temperature rise in the system can easily go beyond the melting temperature of lead thus it could undergo phase transform from solid state to liquid state. Due to that a pressure dependent material model is a better representation of the actual behaviour of the metal rather than strain and strain rate dependent material model (Adams, 2003). Thus in this study *MAT_STEINBERG was used as the material model for the lead fill which is discussed in detail in the next section. This is another material model in LS-DYNA FE code which can be used for high strain rate deformation problems where the strain rates are over $10^5(s^{-1})$. Steinberg et al. (1980) has originally developed the model in which the yield strength is a function of equivalent plastic strain and temperature. This can be used only with the solid elements where an equation of state determines the pressure (Ls Dyna Keyword User's Manual, in Version 971. 2007).

Table 2: Steinburg-Guinan model material parameters for lead

Parameter	*b*	*N*	*B*	*b'*	*h*	*RP*
Value	*110*	*0.52*	*1.160E-10*	*1.160E-10*	*0.00116*	*427.7*

This material model needs to combined with an equation of state in LS-DYNA and Mie-Gruneisen equation of state has used in the current study.

4.3 Mie-Gruneisen Equation of State

The behavior of solids under different pressure and temperature is a key governing factor for this kind of numerical simulations. Gruneisen in 1908 has developed a law which explains the physics that governs the behavior of solids under above mentioned circumstances. The ratio of the coefficient of expansion of a metal to its specific heat at constant pressure is constant at all temperatures (Dulieu-Smith, 1998). It has developed over the years with a concern to get an analytical expression to the law (Adams, 2003; Anderson, 2000). A thermodynamic state of a homogeneous material which is not undergoing any chemical reactions or phase changes may be defined by two state variables is called an equation of state (Ls Dyna Keyword User's Manual, in Version 971. 2007). As described above, the keyword *EOS_GRUNEISEN which is available in the FE code LS-DYNA has selected for this study and used in conjunction with *MAT_STEINBERG keyword.

Table 3: Mie-Gruneisen equation of state parameters for lead

Parameter	*C m/s*	*S1*	*γ*
Value	2051	1.46	2.77

4.4 Fracture Criteria

Using the modified Johnson Cook material model in LS-DYNA the failure of the material can be addressed using two well known criteria. Five parameter Johnson-Cook fracture model (Johnson et al., 1985) and one parameter Cock-Croft and Latham fracture models were considered here.

MJC model used an extended damaged evolution rule where $\dot{D}$ is the damage variable and D_c is the critical damage given by,

$$\dot{D} = \begin{cases} 0 & for\ \varepsilon \leq \varepsilon_d \\ \dfrac{D_c}{\varepsilon_f - \varepsilon_d}\dot{r} & for\ r > \varepsilon_d \end{cases} \tag{11}$$

Where the equivalent fracture strain is given by,

$$\varepsilon_f = \left(D_1 + D_2 \exp\left(-D_3\sigma^*\right)\right)\left(1 + \dot{\varepsilon}^*\right)^{D_4}\left(1 + D_5 T^*\right) \tag{12}$$

D_1-D_5, D_c and ε_d are material constants and shall be obtained from different tests (Ls Dyna Keyword User's Manual, in Version 971. 2007). Over the years this model has used by different researches and has successfully simulated the material failure under similar conditions (Dey et al., 2004) .

Table 4: Johnson-Cook fracture model parameters

Material	*D1*	*D2*	*D3*	*D4*	*D5*
Weldox 460 E	*0.636*	*1.936*	*-2.969*	*-0.014*	*1.014*
Hardened Steel	*0.051*	*0.018*	*-3.00*	*0.0002*	*0.55*

5 Numerical Results

The numerical simulations were performed for different bullet velocities over the range of 300m/s - 1000m/s. Then the residual velocities obtained from the analytical method were compared with numerical simulation results. A part of meshed model is present in the Figure 3 and some plots showing the penetration process shown in Figure 4.

Three element eroding criteria were used in the simulations. When the damage, D is greater than its critical value $D_{c,}$ the element eroded from the analysis. Second criteria used for the element erosion was the critical temperature. Metals subjected to high temperature reduce their load carrying capacity considerably with the increasing temperature (Stouffer et al., 1996). According to the study done by Stouffer and Kane in 1988 on titanium aluminide matrix material ultimate stress of the material has decreased from 600*MPa* to 60*MPa* with the temperature increasing from 21^0C to 982^0C. The melting temperature of the material was 1100^0C. Thus it is clear that at high temperatures, load carrying capacities of the materials are very low. It has assumed that those elements at temperatures closer to melting temperatures can't carry any loads and it is reasonable to delete those elements from the simulation in order to improve the numerical results. Since the aim of this study is not to represent the physical appearance, but to obtain proper ballistic curve for the plate material, T_c=0.5T_m deleting criteria was adopted to prevent element distortion. This also reduces the analysis time by keeping the accuracy within the acceptable range. The third element eroding criteria adopted in this study was the Johnson-Cook fracture criterion which is discussed in section 4.4.

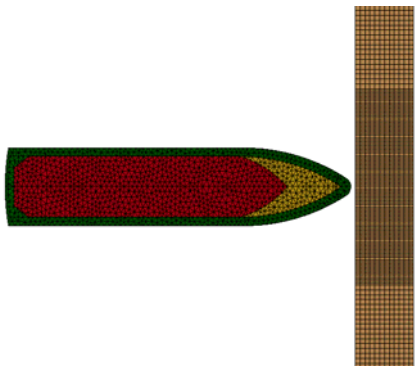

Figure 3: Numerical model of APM2 bullet (half model) with tetrahedral elements and 6mm thick Weldox 460E plate with Hexagonal elements.

Resultant ballistic curve is given in Figure **5**. Chen and Li analytical model for ogive shaped projectiles also plot with the above. It has shown very good correlation between two curves. As a further development of this study, it is planning to compare this result with an existing field tests data. In Chen and Li model, it is assume the projectile as a rigid body. But realistically AMP2 bullet is a deformable body. Inner core with very high strength steel behaves as a rigid body and it also represent more than 80% of the weight of the bullet. Thus it is reasonable to assume it as a semi rigid body and compare the results with Chen and Li model.

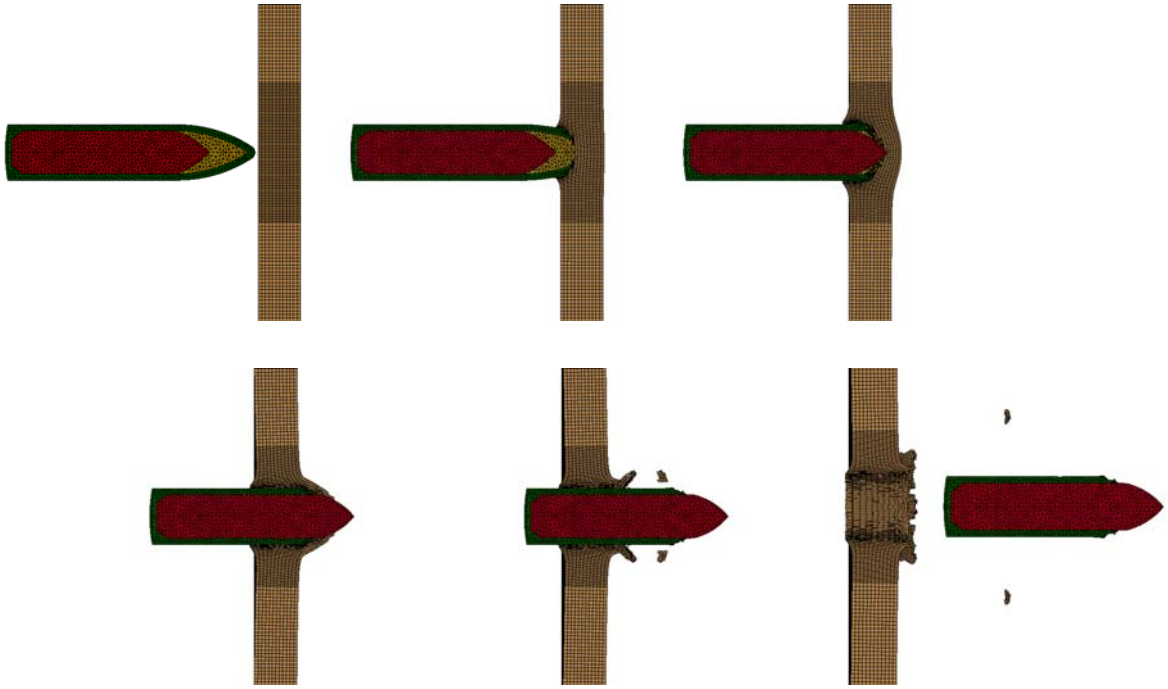

Figure 4: Some plots showing perforation of a 6mm thick Weldox 460E plate by APM2 bullet using Lagrangian Method of LS-DYNA (At incident velocity of 900m/s)

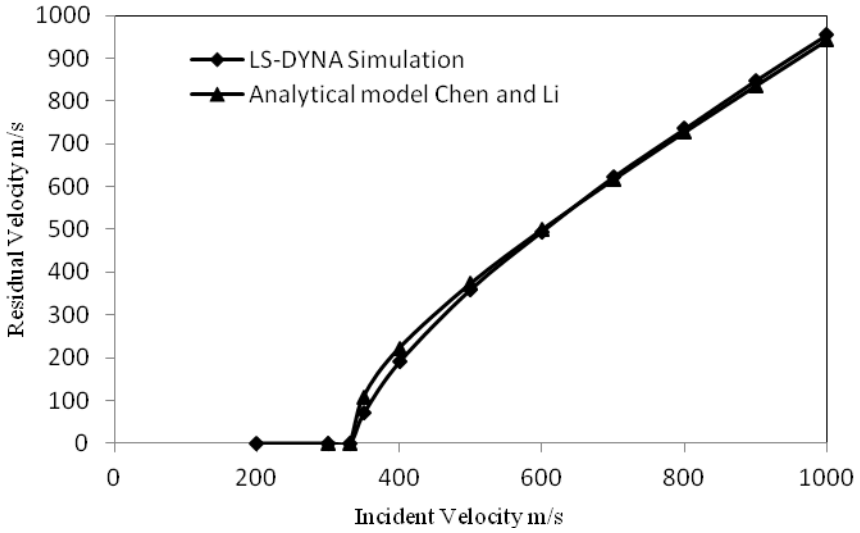

Figure 5: Ballistic limit curves for 6mm thick Weldox 460E plates with APM2 bullets

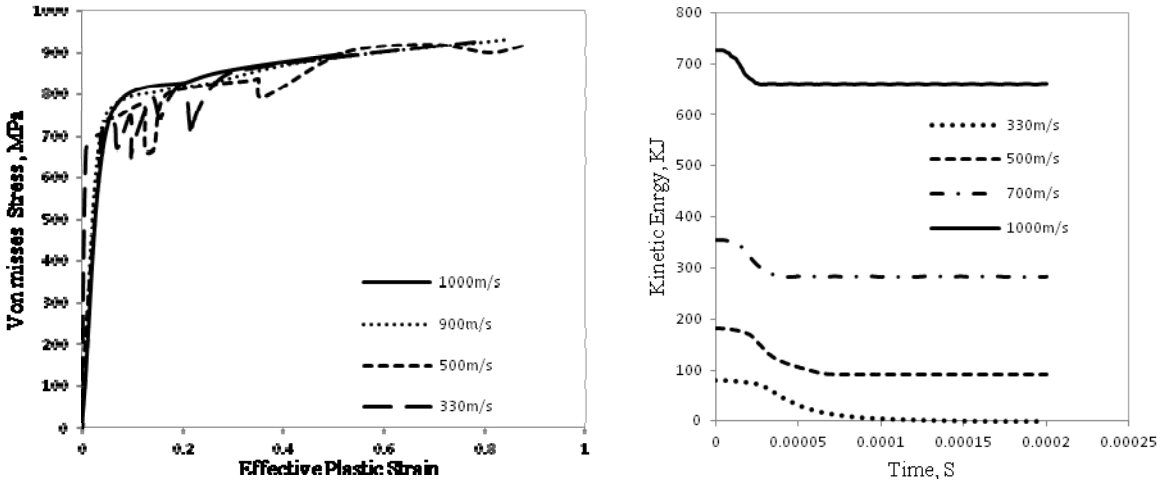

Figure 6: (a) Plastic strain vs Von misses strain curve for a plate element at different velocities (b) Time vs Kinetic energy for the quarter model of the penetrator.

Von misses Stress was obtained for a selected element of the plate and plotted against the effective plastic strain of the element given in Figure 6 (a). For the higher velocities numerical simulations produces smooth curves, but for the lower velocities it's produced some variations. Kinetic energy of the projectile varies largely with the impact velocities. Kinetic energy moves without much variation with time until the projectile hit the plate and rapidly decreases its kinetic energy. Energy decreasing rate at low velocities are less than that of high velocity impacts and shown in Figure 6 (b). This implies more time taken for the penetration process by low velocity impacts.

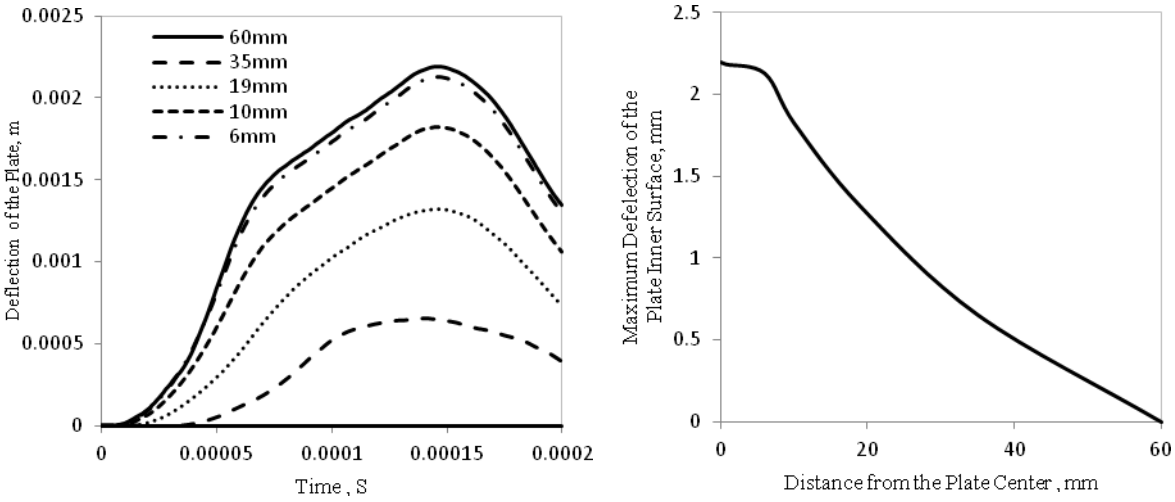

Figure 7: (a) Time vs. Deflection of the Plate at different distances from the plate center (b) Distance from the center of the plate vs. maximum defection of the plate inner surface vi=350m/s.

Deflection of the plate with time is given in the Figure **7**(a) for the projectile impact at 350m/s. Due to the extensive computational time analysis was forced to stop before the full recovery of the elastic deformation. This is the one area which many of the researches haven't addressed and it will be investigated in details in the future works of this study. There are two clearly identifiable regions for the each plot before it reaches it maximum deflection. After it reaches maximum deflection it recovers the elastic deflection rapidly. Figure **7** (b) shows the maximum deflection of the plate for the various distances from the plate center.

6 Conclusion and Discussion

Extensive numerical investigations done using the Lagrangian method available in LS-DYNA shows, it can be used to predict the ballistic limit velocities of the different armour materials with greater accuracy.

The accuracy of the results is mainly depending on the mesh quality of the model, the material parameters and the material models used for the numerical simulations. Tetrahedral element model has also predicted the ballistic limit curve accuracy level required for the armour industry. There is no much difference in analytical time and accuracy of the results was observed between the tetrahedral element model and hexagonal element model.

Local temperature rise is a very important phenomenon in the high strain impact events such as ballistic. Temperature cutoff of 50% of melting temperature has used in the numerical analysis with success. This reduces the computation time and numerical instability by deleting the elements which are going in to semi-liquid state. But in the future of this study will focus on this issue and will investigate the optimum temperature which these elements erosion criteria can be implemented.

References

Børvik, T., S. Deya, and A.H. Clausen, *Perforation resistance of five different high-strength steel plates subjected to small-arms projectiles.* International Journal of Impact Engineering, 2009. 36: p. 948-964.

Chen, X.W. and Q.M. Li, *Perforation of a thick plate by rigid projectiles.* International Journal of Impact Engineering, 2003. 28: p. 743-759.

Horsfall, I., N. Ehsan, and W. Bishop, *A Comparison of the Performance of Various Light Armour Piercing Ammunition.* Journal of Battlefield Technology, 2000. 3: p. 5-8.

G. G Corbett, S. R. Reid, and W. Johnson, *Impact Loading of Plates and Shells by Free-Flying Projectiles: A Review.* International Journal of Impact Engineering, 1996. 18(2): p. 141-230.

Recht, R.F. and T. W. Ipson, *Ballistic perforation dynamics.* journal of Applied Mechanics, 1963. 30: p. 385-391.

Dey, S., et al., *The effect of target strength on the perforation of steel plates using three different projectile nose shapes.* International Journal of Impact Engineering, 2004. 30: p. 1005-1038.

Chen, X.W. and Q.M. Li, *Deep penetration of a non-deformable projectile with different geometrical characteristics.* International Journal of Impact Engineering, 2002. 27: p. 619-637.

Ls Dyna Keyword User's Manual, in *Version 971*. 2007, Livemore Software technology Corporation (LSTC): Califonia,USA.

Odeshi, A.G., S. Al-ameeri, and M.N. Bassim, *Effect of high strain rate on plastic deformation of a low alloy steel subjected to ballistic impact.* Journal of Materials Processing Technology, 2005. 162–163: p. 385–391.

Johnson, G.R. and W.H. Cook, *A constitutive model and data for metal subjected to large strains, high strain rates and high temperature.*

Adams, B., *Simulation of ballistic impacts on armored civil vehicles*. 2003, Eindhoven University of Technology.

Steinberg, D.J., S.G.Cochran, and M.W.Guinan, *A constitutive model for metals applicable at high-strain rate.* Journal of Applied Physics, 1980. 51(3): p. 1498-1504.

Dulieu-Smith, J.M. and P. Stanley, *On the interpretation and significance of the Gru¨neisen parameter in thermoelastic stress analysis.* Journal of Materials Processing Technology, 1998. 78: p. 75-83.

Anderson, O.L., *The Gruneisen ratio for the last 30 years.* Geophys. J. Int., 2000. 173: p. 279-294.

Johnson, G.R. and W.H. Cook, *Fracture characteristics of three metals subjected to various strains, strain rates, temperatures and pressures* Engineering Fracture Mechanics, 1985. 21(1): p. 31-48.

Børvik, T., O.S. Hopperstad, and T. Berstad, *A computational model of viscoplasticity and ductile damage for impact and penetration.* European Journal of Mechanics A/Solids, 2001. 20: p. 685–712.

Børvik, T., O.S. Hopperstad, and T. Berstad, *On the influence of stress triaxiality and strain rate on the behaviour of a structural steel. Part II. Numerical study.* European Journal of Mechanics A/Solids, 2003. 22: p. 15-32.

Børvik, T., et al., *Ballistic penitration of steel plates.* International Journal of Impact Engineering, 1999. 22: p. 855-886.

Stouffer, D.C. and L.T. Dame, *Inelastic Defomation of Metals*. 1996: John Wilkey & Sons,Inc.